Hindawi
Journal of Spectroscopy
Volume 2023, Article ID 7860822, 10 pages
https://doi.org/10.1155/2023/7860822

Research Article

A Dataset on Corn Silage in China Used to Establish a Prediction Model Showing Variation in Nutrient Composition

Shu Zhang,[1] **Jian Hao**,[2] **Donghai Wang**,[1] **Chenglong Luo**,[3] **Na Lu**,[4] **Xiaocen Guo**,[4] **Yanfang Liu**,[5] **Zixiao Zhang**,[4] **and Shengli Li**[3]

[1]*College of Animal Science, Xinjiang Agricultural University, Urumqi 830052, China*
[2]*Inner Mongolia Yili Industrial Group Co.,Ltd., Hohhot 100080, China*
[3]*State Key Laboratory of Animal Nutrition, Beijing Engineering Technology Research Center of Raw Milk Quality and Safety Control, College of Animal Science and Technology, China Agricultural University, Beijing 100193, China*
[4]*Beijing Jingwa Agricultural Science & Technology Innovation Center, Beijing 100193, China*
[5]*Beijing Sino Agricultural Aiko Testing Technology Co.,Ltd., Beijing 100193, China*

Correspondence should be addressed to Zixiao Zhang; 302563508@qq.com and Shengli Li; lisheng0677@163.com

Received 6 April 2023; Revised 30 May 2023; Accepted 8 June 2023; Published 1 July 2023

Academic Editor: Sarfaraz Ahmed Mahesar

It is important to assess the nutritional concentrations of forage before it can be used for tremendous improvements in the dairy industry. This improvement requires a rapid, accurate, and portable method for detecting nutrient values, instead of traditional laboratory analysis. Fourier-transform infrared (ATR-FTIR) spectroscopy technology was applied, and partial least squares regression (PLSR) and backpropagation artificial neural network (BP-ANN) algorithms were used in the current study. The objective of this study was to estimate the discrepancy in nutritional content and rumen degradation in WPCS grown in various regions and to propose a novel analytical method for predicting the nutrient content of whole plant corn silage (WPCS). The Zhengdan 958 cultivar of WPCS was selected from eight different sites to compare the discrepancies in nutrients and rumen degradation. A total of 974 WPCS samples from 235 dairy farms scattered across five Chinese regions were collected, and nutritional indicators were modeled. As a result, substantial discrepancies in nutritional concentrations and rumen degradation of WPCS were found when they were cultivated in different growing regions. The WPCS in Wuxi showed 1.14% higher dry matter (DM) content than that in Jinan. Lanzhou had 11.57% and 8.25% lower neutral detergent fiber (NDF) and acid detergent fiber (ADF) concentrations than Jinan, respectively. The DM degradability of WPCS planted in Bayannur was considerably higher than that in Jinan (6 h degradability: Bayannur vs. Jinan = 49.85% vs. 33.96%), and the starch of WPCS from Bayannur (71.79%) was also the highest after 6 h in the rumen. The results indicated that the contents of NDF, ADF, and starch were estimated precisely based on ATR-FTIR combined with PLSR or the BP-ANN algorithm ($R^2 \geq 0.91$). This was followed by crude protein (CP), DM ($0.82 \leq R^2 \leq 0.90$), ether extract (EE), and ash ($0.66 \leq R^2 \leq 0.81$). The BP-ANN algorithm had a higher prediction performance than PLSR ($R^2_{\text{PLSR}} \leq R^2_{\text{BP-ANN}}$; $\text{RMSE}_{\text{PLSR}} \geq \text{RMSE}_{\text{BP-ANN}}$). The same WPCS cultivar grown in different regions had various nutrient concentrations and rumen degradation. ATR-FTIR technology combined with the BP-ANN algorithm could effectively evaluate the CP, NDF, ADF, and starch contents of WPCS.

1. Introduction

The Chinese dairy industry has developed rapidly over the recent decades and needs to provide milk products for a quarter of the world's population. To adapt to intensive systems, it further requires sustainable supplementation of feedstuffs. A sequence of studies indicates that the nutrient variation of feedstuffs contributes to variation in dairy production [1, 2]. For example, a 13.1% crude protein (CP) diet significantly reduced milk yield to 16.2% CP of the total mixed ration (TMR) in dairy cows [3]. The increase in ether extract (EE) improved the milk fat percentage of dairy cows

[4]. The content of starch (28.5%) owned higher dry matter intake (DMI) and milk yield (MY) than 24% [5]. Thus, it is truly important to detect the nutrient composition before they are utilized.

Whole plant corn silage (WPCS) is the main ingredient in dairy TMR under most dietary regimes, especially for high-yield cows. The corn silage percentage utilized in TMR has contributed to 42% [6]. The extensive use of it could attribute to a high and stable production in conjunction with high contents of total digestible nutrients and metabolizable energy [6–9]. With the exception of genotype and harvest maturity, the yield and nutritional quality of WPSC are highly influenced by environmental conditions [10–12]. For example, high growing temperatures can reduce the digestibility of corn silage because of a substantial increase in lignin content in stovers and a decrease in starch content in the cobs [13, 14]. Moreover, previous studies have reported that precipitation was one of the most influential abiotic factors for plant productivity [15], and drought stress generally contributed to delays in plant growth and development by decreasing cell elongation and reducing photosynthesis [16]. Furthermore, soil moisture and growing temperature were highly related to DM yields because they affected the canopy and anatomical development of maize crops [17]. Above all, it is necessary for dairy farms to detect the nutritional quality of roughage delivered from different frown regions before they are formulated and fed, which provides fundamental information to satisfy the exact nutrient requirements.

Traditional wet chemical analysis requires considerable human, material, and financial resources, and the reagents used would result in environmental pollution [18]. Therefore, the exploration of real-time, efficient, and environmentally friendly techniques has attracted a widespread interest. As a fast, simple, noninvasive, and economical technology, Fourier-transform infrared (ATR-FTIR) spectroscopy can complement or replace existing techniques [19–22]. Using the ATR-FTIR technique, previous studies [23, 24] constructed prediction models for dry matter (DM), CP, neutral detergent fiber (NDF), and acid detergent fiber (ADF) contents in plants. These experiments have predominantly implemented traditional linear regression methods, such as partial least squares regression (PLSR), to build a prediction model between the nutrient contents and spectroscopy information of feedstuffs. But nowadays, the application of artificial neural networks (ANNs) could bring significant improvements in the development of models because of their ability to build complicated and potentially nonlinear relations without any prior assumptions about the underlying data-generating process [25]. A backpropagation artificial neural network (BP-ANN) is the most representative and extensively exploited ANN using the error backpropagation algorithm [26–29]. However, to the authors' knowledge, there is limited information on the application of ATR-FTIR spectroscopy along with PLS and BP-ANN methods to predict the nutrient content of WPCS collected from various grown regions in China.

The objective of this study was to evaluate the between-region differences in nutritive components and rumen degradation of WPCS and to develop rapid and efficient models for predicting nutritional concentrations of WPCS based on ATR-FTIR spectroscopy technology combined with PLSR and BP-ANN algorithms. Simultaneously, a better prediction performance model was selected for further applications.

2. Materials and Methods

2.1. Sample Preparation and Chemical Measurements. The Zhengdan 958 cultivar of WPCS was selected for this study from eight different areas of China, and the location information is shown in Table 1. In each area, three plots were selected, and 20 plants from each plot, 10–15 cm above the ground, were harvested at the kernel maturity stage of the half milk line. The exterior 1 m area of each plot was excluded from sampling to ensure uniformity in the plants being sampled. After harvesting, the corn material from the entire plant was chopped into 2 cm sections and immediately transported to the laboratory. Here, they were prepared by vacuum sealing the inoculated plant material into polyethylene bags (25 × 30 cm). They were then stored in the dark at an ambient temperature until analysis. The filling, compression, and sealing processes were the same for all twenty-four bags.

After 60 d of fermentation, the polyethylene bags were opened, and the samples were collected for the measurement of nutrient concentrations and digestibility. A total of twenty-four subsamples from all the individual bags were dried in a forced-air oven at 65°C for 48 h to determine DM. They were then ground in a Wiley mill (Model no. 2; Arthur H. Thomas Co., Philadelphia, PA) to pass through a 1 mm screen to analyze the chemical composition or through a 4 mm screen to detect the *in situ* nutritive disappearance. The crude protein (CP) was measured using the 988.05 method of the Association of Official Analytical Chemists [30]. Neutral detergent fiber (NDF) and acid detergent fiber (ADF) analyses were performed in an ANKOM 200 fiber analyzer (ANKOM Technologies, Macedon, USA) using thermostable α-amylase [31]. EE was obtained using an automatic extractor (ANKOM XT101; ANKOM Technology Corp., Macedon, NY, USA). Ash was determined by combustion at 600°C for 6 h in a furnace according to method no. 924.05 [32]. The starch content was analyzed using a total starch assay kit (Megazyme, Bray, Ireland; method no. 996.11) based on the AOAC method [32].

2.2. Animals and Digestible Measurements. Three healthy Holstein dairy cows (139 ± 15 days in milk, 2.50 ± 0.50 parity) fixed with permanent rumen fistula from the experimental base of China Agricultural University were used for the *in situ* incubation study. The trial procedure was submitted to the Experimental Animal Welfare and Animal Ethics Committee of China Agricultural University (approval no. CAU2021009−2). The animals were fed TMR with a forage-to-concentrate ratio of 60: 40, twice daily at 07:00 h and 21:00 h. The TMR components and nutrient levels are shown in Table 2. Subsamples (ca.7 g) were randomly

Table 1: Planting region information of corn silage from the entire plant.

Site grown	Longitude and latitude	Sample number	Sample time
Jinan	E 117°01′; N 36°65′	60	2018.08.01–2019.08.02
Liaoning	E 123°25′; N 41°48′	60	2018.08.04–2019.08.05
Lanzhou	E 103°40′; N 36°03′	60	2018.08.08–2019.08.09
Ningxia	E 105°50′; N 38°17′	60	2018.08.10–2019.08.11
Zhangjiakou	E 114°52′; N 40°47′	60	2018.08.14–2019.08.15
Bayannur	E 107°6′; N 40°34′	60	2018.08.17–2019.08.18
Durbert	E 123°47′; N 45°23′	60	2018.08.20–2019.08.22
Wuxi	E 119°33′; N 31°07′	60	2018.08.25–2019.08.26

Table 2: Composition and nutrient levels of the basal diet.

Ingredients	Contents %	Nutrient level	Contents %
Corn silage	25.13	DM	93.9
Corn	15.53	CP	17.30
Alfalfa hay	15.08	EE	5.01
Flaked corn	7.92	NDF	32.69
Soybean meal	7.88	ADF	20.23
Beet granules	5.77	Starch	24.42
Cotton seed	4.53	Ca	0.81
Brewer's grain	4.02	*P*	0.43
DDGS	3.41	NE_L/(MCal/kg)[2]	1.75
Cotton meal	2.93		
Oat hay	1.9		
Extruded soybeans	1.84		
$NaHCO_3$	1.13		
Limestone	0.83		
Rumen-pass fatty acid	0.63		
Premix[1]	0.41		
$CaHPO_4$	0.29		
MgO	0.28		
$KHCO_3$	0.21		
Salt	0.21		
Yeast culture	0.07		

[1]One kilogram of premix contained the following: VA 200kIU, VD 60kIU, VE 1400IU, Cu (as copper sulfate) 520 ppm, Mn 760 ppm, Zn 2400 ppm, I 40 ppm, Se 15 ppm, Co 10 ppm, and Fe 400 ppm (Cargill Co., Ltd.). [2]NEL, net energy of lactation, a value calculated according to NRC 2001, while the other nutrient contents were measured values.

incubated in sealed nylon bags (10 × 20 cm, pore size 40 μm) in the rumen of fistulated cows for 6, 24, 30, and 48 h, using the "gradual in/all out" schedule. Starch digestibility after 6 h of incubation and NDF digestibility after 30 h of incubation were associated with the value and quality of feedstuff [33, 34]. Three replicate bags per sample from individual cows were used at each incubation time point. After incubation, all the nylon bags were removed from the rumen, washed with cold running tap water six times, and then dried to constant weight in forced air at 65°C. The dried residues of the replicate bags of each sample were pooled and mixed according to the incubation time, ground, and stored in sealed plastic bags for further analysis. The rumen degradation characteristics were calculated using the following formula [35, 36]:

$$\text{Degradation rate} = \frac{\text{nutrient content} \times \text{sample weight} - \text{nutrient content} \times \text{residue weight}}{\text{nutrient content} \times \text{sample weight}} \times 100\%. \quad (1)$$

2.3. Sample Preparation, ATR-FTIR Spectra Analysis, and Model Building. To establish stable and precious predictive models of nutritional components (DM, CP, EE, ash, NDF, ADF, starch, Ca, and P), 974 WPCS samples (43 cultivars) were collected from more than 200 dairy farms located in Beijing, Tianjin, Ningxia, Inner Mongolia, Shandong, Heilongjiang, and some other sites. The relative information of these samples is shown in Table 3. The physical parameters of fresh plants, including whole-plant height and weight, kernel number, ear number, and weight, were measured immediately at harvest, and the emergence rate was calculated later. All the samples selected were chopped into

Table 3: Planting region information of samples for prediction.

Area grown	City (sample number)	Total number	Sample time
Northeast region	Harbin (196) Shenyang (191)	287	2019.08.12–2019.08.20
Northwest region	Yinchuan (65) Lanzhou (73)	138	2019.09.02–2019.09.07
North China	Beijing (99) Tianjin (81) Baotou (85)	265	2019.09.21–2019.09.30
East China	Jinan (121) Nanjing (77)	198	2019.10.23–2019.10.29
Southwest region	Chengdu (86)	86	2019.11.11–2019.11.13

small particles (1–2 cm) and transported to the laboratory, where they were ground through a 1.0 mm screen for chemical analysis, or a 0.25 mm screen for molecular spectral analysis.

ATR-FTIR spectra were acquired using a Fourier-transform spectrometer (FOSS-DS-2500, FOSS Analytical SA, DK 3400 HillerØed, Denmark). Two grams of each crushed WPCS powder was placed into a glass sample. During each scanning procedure, the ATR-FTIR spectra were recorded with a wavelength in the range of 800–2500 nm at 1 nm intervals, and 32 scans at a resolution of 8 cm^{-1} were taken per side and averaged into a single spectrum. Each sample was scanned three times, and the average value was used for spectrum analysis. The spectral absorbance values were obtained as log $1/R$, where R is the sample reflectance. The raw ATR-FTIR spectra of the 974 samples are shown in Figure 1.

Raw spectra measured using the ATR-FTIR spectrometer included noise and extra background information in addition to sample information. Therefore, preprocessing of spectral data before calibration of a reliable, accurate, and stable model was necessary. In the current study, mean centering was applied to the spectral preprocess. A principal component analysis (PCA) model was used to detect outliers and reduce the dimensions of spectral data in the WPCS samples through principal components and scores (PCs) [27].

The PLSR algorithm implemented in Unscrambler X 10.4 software (CAMO Software AS, Oslo, Norway) was used to establish a predictable model. A three-layer structure (input, hidden, and output layers) BP-ANN implemented in MATLAB R2019a (MathWorks Inc., Natick, MA, USA) was used as another predictable model [37]. To assess the efficiency of the multivariate calibration models, two statistical parameters, root mean square error of calibration (RMSEC) and root mean square error of prediction (RMSEP), were calculated according to the following equations (27):

$$\mathrm{RMSEC} = \sqrt{\frac{\sum_{i=1}^{n}(yi - \hat{yi})^2}{n_c}},$$
$$\mathrm{RMSEP} = \sqrt{\frac{\sum_{i=1}^{n}(yi - \hat{yi})^2}{n_p}}, \quad (2)$$

where yi and $\hat{yi}$ are the predicted and measured values (nutrient content of the WPCS), respectively.

The correlation coefficients for calibration (R^2c) and prediction (R^2p) are generally used to evaluate the correlation between the results:

$$\mathrm{R}^2 = \left[1 - \frac{\sum_{i=1}^{n}(yi - \hat{yi})^2}{\sum_{i=1}^{n}(yi - \overline{y})^2}\right] \times 100\%, \quad (3)$$

where $\overline{\mathbf{y}}$ is the average measurement of the WPCS samples and n denotes the number of WPCS samples in the dataset. A model with high R^2 and low RMSEC demonstrated superior performance [30]. The model may be used for crude prediction if $0.66 \le \mathrm{R2} \le 0.81$, more accurate prediction if $0.82 \le \mathrm{R2} \le 0.90$, or normal analysis if $\mathrm{R2} \ge 0.91$ [31].

2.4. Statistical Analysis. Data on nutritional components and rumen degradation kinetic parameters were analyzed using one-way ANOVA in SAS 9.2 software (SAS Institute, Cary, NC, USA). The Duncan method was used to analyze the multiple comparisons based on the following model:

$$Y_{ijk} = \mu + T_i + D_j + e_{ijk}, \quad (4)$$

where Y_{ijk} represents the nutritional components and real-time degradable rate, μ is the overall average, and T_i represents the different growing regions of alfalfa hay, D_j is the random effect, and e_{ijk} is the model error.

For all the statistical analyses, a significant difference was declared at $P < 0.05$, whereas a tendency was identified at $0.05 \le P \le 0.1$.

3. Results and Discussion

3.1. Effects of Nutritional Contents and Rumen Degradation of WPCS Grown in Different Regions. As the main roughage source of ruminant feedstuffs, nutritional content and rumen degradability have attracted widespread attention. According to Table 4, except for CP, the nutrient components of WPCS, including DM, NDF, ADF, EE, ash, and starch of WPCS, varied considerably in different regions. WPCS grown in Wuxi had the highest DM content (93.89%), whereas Jinan (92.48%) had the lowest. Meanwhile, the highest NDF (47.19%) and ADF (26.77%) concentrations of WPCS were observed when they were cultivated in Jinan. The city of Ningxia had the highest EE

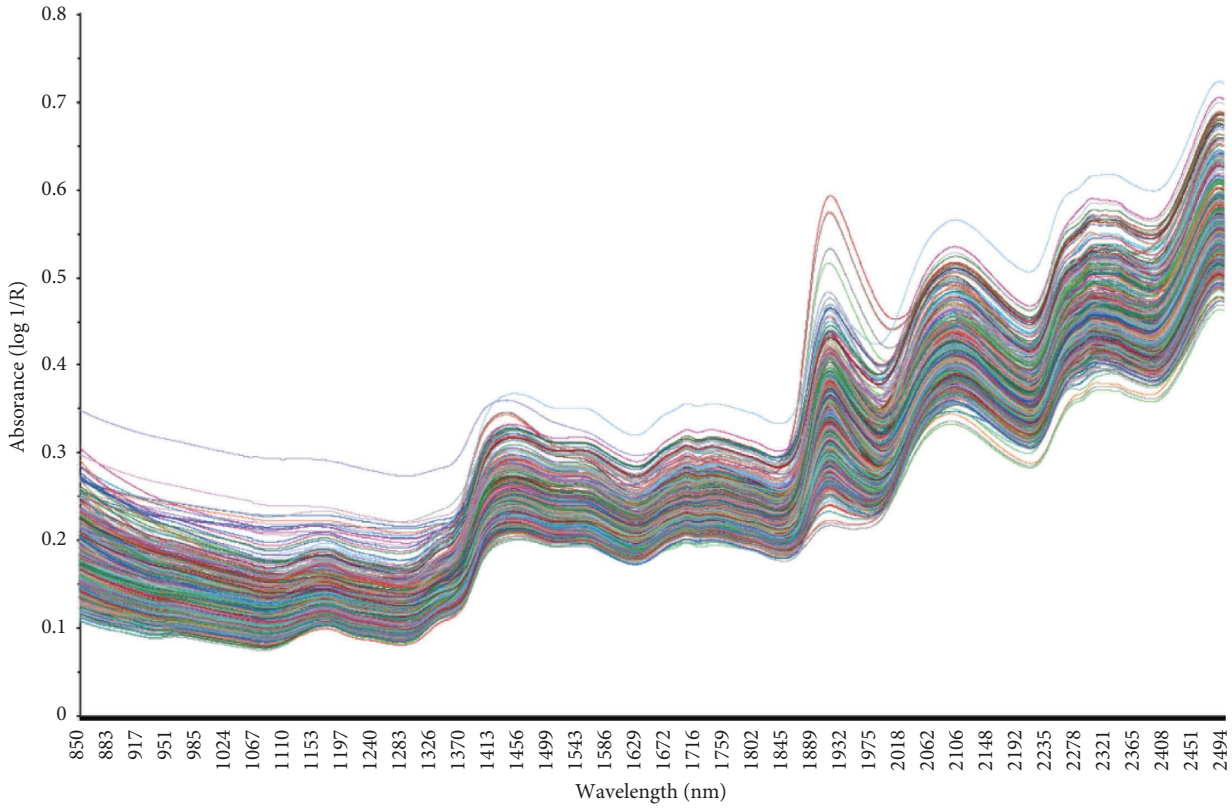

Figure 1: Original spectrum of whole plant corn silage.

Table 4: The nutritional contents of whole plant corn silage (DM basis) %.

Items	DM	CP	NDF	ADF	EE	Ash	Starch
Jinan	92.48 ± 0.14^{c}	7.81 ± 0.52	47.19 ± 0.92^{a}	26.77 ± 0.13^{a}	3.10 ± 0.10^{ab}	4.44 ± 0.12^{a}	28.15 ± 0.84^{a}
Liaoning	93.78 ± 0.01^{ab}	6.94 ± 1.96	35.49 ± 0.98^{c}	18.5 ± 0.79^{e}	2.33 ± 0.61^{c}	3.96 ± 0.05^{b}	28.58 ± 0.59^{a}
Lanzhou	93.64 ± 0.45^{ab}	7.77 ± 0.62	35.62 ± 0.47^{c}	18.52 ± 0.30^{e}	$3.05 \pm 0.08a^{bc}$	3.37 ± 0.03^{d}	27.99 ± 0.43^{ab}
Ningxia	93.48 ± 0.02^{ab}	7.73 ± 1.58	40.6 ± 2.22^{b}	21.87 ± 1.39^{c}	3.32 ± 0.03^{a}	4.41 ± 0.03^{a}	27.81 ± 0.46^{ab}
Zhangjiakou	93.37 ± 0.06^{b}	7.99 ± 0.36	34.52 ± 0.88^{c}	24.87 ± 0.49^{b}	2.78 ± 0.04^{abc}	3.99 ± 0.05^{b}	26.79 ± 0.12^{bc}
Bayannur	93.4 ± 0.06^{b}	7.19 ± 0.56	36.7 ± 1.00^{c}	20.65 ± 0.62^{cd}	3.17 ± 0.52^{ab}	3.6 ± 0.03^{c}	27.8 ± 0.49^{ab}
Durbert	93.48 ± 0.12^{ab}	7.05 ± 0.66	33.62 ± 2.42^{c}	19.94 ± 0.59^{de}	2.83 ± 0.13^{abc}	3.25 ± 0.06^{d}	26.27 ± 0.83^{cd}
Wuxi	93.89 ± 0.03^{a}	6.77 ± 0.62	35.76 ± 0.83^{c}	19.4 ± 0.41^{de}	2.55 ± 0.08^{bc}	4.08 ± 0.01^{b}	25.17 ± 0.39^{d}

(3.32%), while Liaoning represented the opposite condition (2.33%). These results imply that climate conditions such as precipitation and growing temperature can affect internal nutrient accumulation in WPSC [38]. Higher soil pH accelerates the deposition of fatty acids in plants [39]. This means that the different EE contents of WPCS may be the result of soil salinity.

The WPCS from Jinan and Ningxia had higher ash content than that from Lanzhou and Durbert. This result may have contributed to the discrepancy in smooth harvesting ground. More soil was taken into the feedstuffs, and higher ash content was detected when ground flatness was poor. Starch is one of the main factors that influence cow milking performance [40–42]. The results related to starch content in our study have verified that alfalfa hay grown in northeast China may have a greater milking quality.

Figure 2 shows that the DM degradability of WPCS planted in Bayannur was substantially higher than that in Jinan. The starch content of WPCS from Bayannur was also the highest after 6 h in the rumen. The difference in rumen degradation among various regions could be explained by the effective area of rumen microbial invasion to feed and the protein structure [36, 37]. The passage rate of digestation through the foreign stomachs is triggered by particle size, rumen washout, rumen wall distension, or papillae tactile signals that also occur in the different results [43]. Sugar digestibility may be another reason that led to the discrepancy [44], and it is worth investigating in the future. In the current study, the 6 h and 48 h rumen degradation of NDF and ADF in WPCS from different regions reflected their various nutritional uses [45].

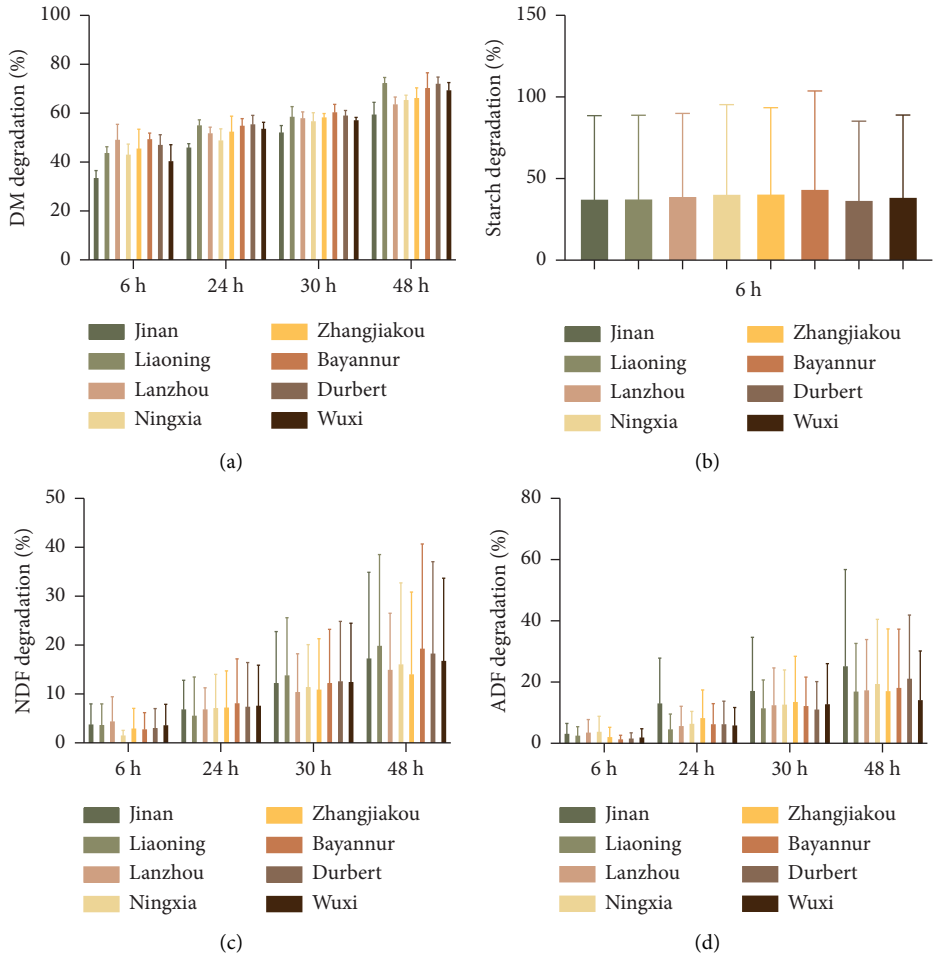

Figure 2: Rumen degradable characteristics of nutrients in whole plant corn silage: (a) DM degradation; (b) starch degradation; (c) NDF degradation; (d) ADF degradation.

3.2. Establishment and Validation of the PLSR Model. The substantial variation in nutritional indices and rumen degradation indicated that it was necessary to evaluate the nutrients in roughage before they were priced, formulated, and used. However, traditional chemical methods not only consume human, material, and financial resources but also contribute to a potential environmental pollution caused by reagents [18], which deviates from dairy farming profits and is inconsistent with sustainable development. The conventional method resulted in some errors owing to different experimenters and instruments. Therefore, a rapid, efficient, and environment-friendly technique needs to be explored. ATR-FTIR technology has expanded considerably worldwide because of its ability for field or online applications and its simultaneous evaluation of large amounts of samples over relatively short timescales. Therefore, 43 WPCS cultivars from over 200 dairy farms located in five Chinese regions were collected to establish a model for predicting nutrients.

As shown in Table S1, a high variable coefficient (CV) was calculated, especially the contents of Ca (33.58%), ash (24.08%), and starch (23.64%), which were followed by ADF (16.25%), EE (16.07%), P (15.74%), NDF (14.41%), CP (12.62%), and DM (1.83%). This substantial range of variation demonstrated that the WPCS samples ($n = 974$) were broadly representative. The variations in rumen degradation and morphological characteristics are shown in Tables S2 and S3.

PLSR is the most commonly used regression method for quantitative analysis of the ATR-FTIR spectrum [46]. In this study, cross-validation was performed on the calibration set to select the optimal factors for the PLSR model [22]. With the growth of the factors, the ascensional range of the explained variance becomes relatively small. The closer the explained value is to 1, the higher the accuracy of the constructed model. However, a wide gap between the calibration and prediction sets would be observed if many factors contributed to overfitting [25]. Therefore, the selection of a strategic number of factors is more conducive to the establishment of an optimum model. All the WPCS was sorted randomly into N counterparts. Each part had similar numbers and accounted for approximately 5% of the total samples. Subsequently, one out of N was removed as the prediction set, and the remaining samples were used as the calibration set (for more details on the PLSR models, please refer to Xing et al. [47]). RMSE and R^2 were used as parameters to select the optimal calibration model, which was

then applied to the prediction set. The smaller the RMSE and the bigger the R^2, the greater the prediction performance of the model [48].

A summary of the optional factor number of different nutrients in WPCS, in conjunction with the calibration and prediction results, is shown in Table 5 and Figure S1. The PLSR model developed showed excellent prediction performance for NDF, ADF, and starch of WPCS samples, with R^2c of 0.910, 0.921, and 0.933 and R^2p of 0.904, 0.916, and 0.929, respectively. Our results were partially similar to those of Werbos et al.[49], who constructed optimal prediction models for NDF and ADF. The reason for this similar phenomenon may be explained by the high contents of NDF and ADF. The existence of hydrogen-containing groups in them produced pronounced absorption peaks in the near-infrared region. ANKOM 2000i (ANKOM Technology, USA) was used for the measurement of NDF and ADF, and six parallel replicates ensured the accuracy of the analysis. However, He et al. [24] reported that the predictive performance of NDF and ADF contents was lower than that of other nutritional items. This may be related to the source and number of samples, in conjunction with the ATR-FTIR sensitivity as well as the chemical determination accuracy [50].

A strong performance for predicting DM and CP was displayed with R^2c values of 0.836 and 0.903 and R^2p values of 0.823 and 0.900, respectively. Then, EE and ash were tested according to values of R^2c of 0.788 and 0.795, and R^2p of 0.763 and 0.799, respectively. Anyway, the value of R^2 obtained in the current study is usable for screening and most applications according to Williams [51]. However, neither Ca nor P could be forecasted based on the available data because of the low values of R^2. A likely explanation for this is the lack of ATR-FTIR absorption features for minerals which may be related to water absorption bands [22]. It means that the potential limitations and drawbacks of ATR-FTIR technology, such as its inability to accurately assess certain nutrients, are not adequately addressed, and it is worth searching further.

3.3. Establishment and Validation of the BP-ANN Model. The BP algorithm was initially proposed by Werbos [52], and its application for the training of ANN was popularized by Niu et al. [53]. Working as neurons in the brain, the BP-ANN model is a powerful intelligent chemometric method for data processing [28]. The working principle of BP-ANN was introduced by Pérez–Marín et al. [29]. In this study, 974 WPCS samples were classified into calibration and prediction sets according to a ratio of 9:1. A total of 877 calibrations and 97 prediction set samples were obtained. Before BP training, some parameters were set as follows: 20 principal components were used as input layers because they explained more than 99% and close to 100% of the population variability. The transfer function of the hidden layer was transient, and the node number of the hidden layer was 6. The transfer function of the output layer used purelin, and the note number of the output layer was 1. The algorithm of LM (Levenberg–Marquardt) and ADAPT gradient descent momentum learning function were employed for model training; the training speed was 0.001.

Table 5: Performance of the PLSR model for prediction of nutrient contents in whole plant corn silage.

Nutrition index	Factors	Calibration set		Prediction set	
		R^2c	RMSEC	R^2p	RMSEP
DM	12	0.836	0.675	0.823	0.701
CP	11	0.903	0.407	0.900	0.418
EE	13	0.788	0.261	0.763	0.276
Ash	14	0.795	0.543	0.779	0.564
NDF	13	0.921	1.756	0.916	1.813
ADF	13	0.910	1.281	0.904	1.321
Starch	13	0.933	1.952	0.929	2.004
Ca	7	0.418	0.0615	0.376	0.064
P	10	0.499	0.029	0.477	0.030

[1]Factors: the optimal number of factors used in the PLSR model.

Table 6: The performance of the BP-ANN model for prediction of nutrient contents in whole plant corn silage.

Nutrition index	Factors	Calibration set		Prediction set	
		R^2c	RMSEC	R^2p	RMSEP
DM	20	0.900	0.550	0.845	0.642
CP	20	0.945	0.293	0.927	0.519
EE	20	0.886	0.420	0.853	0.579
Ash	20	0.902	0.806	0.847	0.792
NDF	20	0.965	0.650	0.935	0.627
ADF	20	0.991	0.667	0.975	0.993
Starch	20	0.972	0.763	0.944	0.761
Ca	20	0.730	0.806	0.509	0.792
P	20	0.615	0.806	0.453	0.792

[1]Factors: the optimal number of factors used in the BP-ANN model.

The measured and predicted values of the nutrient content in the WPCS are shown in Figure S2. Table 6 shows the evaluation parameters of the BP-ANN model. These results indicate that the BP-ANN model exhibited excellent prediction performance for CP ($R^2c = 0.945$; $R^2p = 0.927$), NDF ($R^2c = 0.965$; $R^2p = 0.935$), ADF ($R^2c = 0.991$; $R^2p = 0.975$), and starch ($R^2c = 0.972$; $R^2p = 0.944$). The indicators of DM ($R^2c = 0.900$; $R^2p = 0.845$), EE ($R^2c = 0.886$; $R^2p = 0.853$), and ash ($R^2c = 0.902$; $R^2p = 0.847$) were also well predicted. However, poor prediction performance was observed for Ca ($R^2c = 0.730$; $R^2p = 0.509$) and P ($R^2c = 0.615$; $R^2p = 0.453$). The acquisition of successful prediction models, especially NDF, ADF, and starch, may be a result of large samples obtained from five Chinese regions that expressed an extensive geographical span. ATR-FTIR is a typical indirect analytical technique, and its veracity is strongly associated with the precision and accuracy of conventional chemical measurements. In addition, we need to continuously enlarge samples and upload data in the system to guarantee predictive accuracy.

3.4. Performance Evaluation of the PLSR and BP-ANN Multivariate Calibration Methods. The evaluation parameters for the comparison of the PLSR and BP-ANN models are shown in Table 7. The BP-ANN model exhibited more effective prediction performance for the nutrient content of

Table 7: Comparison of performance of PLSR and the BP-ANN algorithm for predicting nutrient contents of whole plant corn silage.

Nutrition index	Model	Calibration set		Prediction set	
		R^2c	RMSEC	R^2p	RMSEP
DM	PLSR	0.836	0.675	0.823	0.701
	BP-ANN	0.900	0.550	0.845	0.642
CP	PLSR	0.903	0.407	0.900	0.418
	BP-ANN	0.945	0.293	0.927	0.519
EE	PLSR	0.788	0.261	0.763	0.276
	BP-ANN	0.886	0.420	0.853	0.579
Ash	PLSR	0.795	0.543	0.779	0.564
	BP-ANN	0.902	0.806	0.847	0.792
NDF	PLSR	0.921	1.756	0.916	1.813
	BP-ANN	0.965	0.650	0.935	0.627
ADF	PLSR	0.910	1.281	0.904	1.321
	BP-ANN	0.991	0.667	0.975	0.993
Starch	PLSR	0.933	1.952	0.929	2.004
	BP-ANN	0.972	0.763	0.944	0.761
Ca	PLSR	0.418	0.061	0.376	0.064
	BP-ANN	0.730	0.806	0.509	0.792
P	PLSR	0.499	0.029	0.477	0.030
	BP-ANN	0.615	0.806	0.453	0.792

WPCS than the PLSR model because of the higher R^2c and R^2p in conjunction with lower RMSEC and RMESP values. These were strongly influenced by the flexibility of the BP-ANN method. BP-ANN could determine the linear and nonlinear relationships between the ATR-FTIR spectrum data and the corresponding physicochemical attributes [28]. The use of BP-ANN reduced the training time and provided higher computational efficiency than the PLSR method.

4. Conclusions

In conclusion, the nutrient composition and rumen degradation of WPCS grown in different regions showed substantial discrepancies. Based on the representative data, ATR-FTIR technology is utilized and considered as an efficient and simple tool for predicting nutritional components of WPCS, which not only quickly optimizes feed formulation but also improves the productivity of the dairy industry. Furthermore, the application of the BP-ANN algorithm could contribute to marked improvements in the models developed and finally can supply a more rapid and reliable model because of its self-learning, self-organizing, strong fault-tolerating, and adapting high nonlinear computing abilities. Finally, extensive samples of WPCS were collected from different regions and dairy farms to improve the robustness and universality of the present study, which also enhanced the practical applicability of the models we explored.

Data Availability

The data used to support the findings of this study are available from the corresponding author upon request.

Conflicts of Interest

The authors declare that they have no conflicts of interest.

Authors' Contributions

S.L. and Z.Z. conceptualized the study. S.Z. developed the methodology. D.W. developed the software. S.L. and S.Z. validated the data. S.Z. performed the formal analysis. S.Z., J.H., D.W., and C.L. investigated the data. J.H. collected the resources. N.L. curated the data. S.Z. wrote and prepared the original draft. Y.L. and X.G. wrote, reviewed, and edited the data. Y.L. visualized the study. S.L. supervised the study. Z.Z. administered the project. S.L. acquired the funds. All authors have read and agreed to the published version of the manuscript.

Acknowledgments

The authors would like to thank the China Agriculture Research System of MOF and MARA, in conjunction with the support of modern farming for this experiment. This research was supported by the Earmarked Fund for CARS36.

Supplementary Materials

Figure S1: distribution of predicted and measured nutrient contents of whole plant corn silage based on the PLSR model. Figure S2: distribution of predicted and measured nutrient contents of whole plant corn silage based on the BP-ANN model. Table S1: the nutrient contents and variation ranges of whole plant corn silage. Table S2: the rumen degradation and variation ranges of whole plant corn silage. Table S3: morphological measurements of different cultivars of whole plant corn silage. (*Supplementary Materials*)

References

[1] N. P. Martin, M. P. Russelle, J. M. Powell et al., "Invited review: sustainable forage and grain crop production for the US dairy industry," *Journal of Dairy Science*, vol. 100, no. 12, pp. 9479–9494, 2017.

[2] T. Senga Kiessé, M. S. Corson, and A. Wilfart, "Analysis of milk production and greenhouse gas emissions as a function of extreme variations in forage production among French dairy farms," *Journal of Environmental Management*, vol. 307, Article ID 114537, 2022.

[3] T. Barros, M. A. Quaassdorff, M. J. Aguerre et al., "Effects of dietary crude protein concentration on late-lactation dairy cow performance and indicators of nitrogen utilization," *Journal of Dairy Science*, vol. 100, no. 7, pp. 5434–5448, 2017.

[4] B. C. Venturelli, J. E. de Freitas Júnior, C. S. Takiya et al., "Total tract nutrient digestion and milk fatty acid profile of dairy cows fed diets containing different levels of whole raw soya beans," *Journal of Animal Physiology and Animal Nutrition*, vol. 99, no. 6, pp. 1149–1160, 2015.

[5] P. N. Gott, J. S. Hogan, and W. P. Weiss, "Effects of various starch feeding regimens on responses of dairy cows to intramammary lipopolysaccharide infusion," *Journal of Dairy Science*, vol. 98, no. 3, pp. 1786–1796, 2015.

[6] L. F. Ferraretto and R. D. Shaver, "Effects of whole-plant corn silage hybrid type on intake, digestion, ruminal fermentation,

and lactation performance by dairy cows through a meta-analysis," *Journal of Dairy Science*, vol. 98, no. 4, pp. 2662–2675, 2015.

[7] K. T. Khaing, T. C. Loh, S. Ghizan, R. A. Halim, and A. A. Samsudin, "Feed intake, growth performance and digestibility in goats fed whole corn plant silage and Napier grass," *Malaysian Journal of Animal Science*, vol. 18, no. 1, pp. 87–97, 2015.

[8] N. A. Khan, T. A. Tewoldebrhan, R. L. G. Zom, J. W. Cone, and W. H. Hendriks, "Effect of corn silage harvest maturity and concentrate type on milk fatty acid composition of dairy cows," *Journal of Dairy Science*, vol. 95, no. 3, pp. 1472–1483, 2012.

[9] N. A. Khan, P. Yu, M. Ali, J. W. Cone, and W. H. Hendriks, "Nutritive value of maize silage in relation to dairy cow performance and milk quality," *Journal of the Science of Food and Agriculture*, vol. 95, no. 2, pp. 238–252, 2015.

[10] S. Abeysekara, N. A. Khan, and P. Yu, "Relationship between protein molecular structural makeup and metabolizable protein supply to dairy cattle from new cool-season forage corn cultivars," *Spectrochimica Acta Part A: Molecular and Biomolecular Spectroscopy*, vol. 191, pp. 303–314, 2018.

[11] T. F. Bernardes, J. L. P. Daniel, A. T. Adesogan et al., "Silage review: unique challenges of silages made in hot and cold regions," *Journal of Dairy Science*, vol. 101, no. 5, pp. 4001–4019, 2018.

[12] L. Kung, R. D. Shaver, R. J. Grant, and R. J. Schmidt, "Silage review: interpretation of chemical, microbial, and organoleptic components of silages," *Journal of Dairy Science*, vol. 101, no. 5, pp. 4020–4033, 2018.

[13] S. B. Temime, E. Campeol, P. L. Cioni, D. Daoud, and M. Zarrouk, "Volatile compounds from Chétoui olive oil and variations induced by growing area," *Food Chemistry*, vol. 99, no. 2, pp. 315–325, 2006.

[14] K. Rengsirikul, Y. Ishii, K. Kangvansaichol et al., "Biomass yield, chemical composition and potential ethanol yields of 8 cultivars of napiergrass (Pennisetum purpureum schumach.) harvested 3-monthly in Central Thailand," *Journal of Sustainable Bioenergy Systems*, vol. 3, no. 2, pp. 107–112, 2013.

[15] T. E. Huxman, M. D. Smith, P. A. Fay et al., "Convergence across biomes to a common rain-use efficiency," *Nature*, vol. 429, no. 6992, pp. 651–654, 2004.

[16] J. A. Polania, V. Salazar-Chavarría, I. Gonzalez-Lemes, A. Acosta-Maspons, C. C. C. Chater, and A. A. Covarrubias, "Contrasting phaseolus crop water use patterns and stomatal dynamics in response to terminal drought," *Frontiers in Plant Science*, vol. 13, Article ID 894657, 2022.

[17] E. Habermann, J. A. B. San Martin, D. R. Contin et al., "Increasing atmospheric CO_2 and canopy temperature induces anatomical and physiological changes in leaves of the C_4 forage species Panicum maximum," *PLoS One*, vol. 14, no. 2, Article ID e0212506, 2019.

[18] G. Tao, *Study on Prediction of Nutrient Composition of Straw and Alfalfa hay Using NIRS Technology*, Lanzhou University, Lanzhou, China, 2020.

[19] Z. Guo, A. O. Barimah, A. Shujat et al., "Simultaneous quantification of active constituents and antioxidant capability of green tea using NIR spectroscopy coupled with swarm intelligence algorithm," *Lebensmittel-Wissenschaft & Technologie*, vol. 129, Article ID 109510, 2020.

[20] E. A. Macavilca and L. Condezo-Hoyos, "Assessment of total antioxidant capacity of altiplano colored quinoa (Chenopodium quinoa willd) by visible and near-infrared diffuse reflectance spectroscopy and chemometrics," *Lebensmittel-Wissenschaft & Technologie*, vol. 134, Article ID 110182, 2020.

[21] R. Zimmerleiter, J. Kager, R. Nikzad-Langerodi et al., "Probeless non-invasive near-infrared spectroscopic bioprocess monitoring using microspectrometer technology," *Analytical and Bioanalytical Chemistry*, vol. 412, no. 9, pp. 2103–2109, 2020.

[22] G. Buonaiuto, D. Cavallini, L. M. E. Mammi et al., "The accuracy of NIRS in predicting chemical composition and fibre digestibility of hay-based total mixed rations," *Italian Journal of Animal Science*, vol. 20, no. 1, pp. 1730–1739, 2021.

[23] N. N. Xiang, J. T. Zhao, L. Chen et al., "Research on evaluation of fiber content in soybean hulls based on near-infrared spectroscopy technique," *Journal of Animal Nutrition (in Chinese)*, vol. 33, no. 3, pp. 1792–1800, 2020.

[24] Y. He, L. Zhang, X. J. Wu et al., "Near infrared prediction model establishment for routine nutritional component contents of alfalfa hay," *Journal of Animal Nutrition (in Chinese)*, vol. 31, no. 10, pp. 4684–4690, 2019.

[25] L. J. Chen, L. Xing, and L. J. Han, "Quantitative determination of nutrient content in poultry manure by near infrared spectroscopy based on artificial neural networks," *Poultry Science*, vol. 88, no. 12, pp. 2496–2503, 2009.

[26] X. Hua, G. Zhang, J. W. Yang, and Z. Y. Li, "Theory study and application of the BP-ANN method for power grid short-term load forecasting," *ZTE Communications*, vol. 13, no. 3, pp. 2–5, 2015.

[27] S. Zandbaaf, M. Reza Khanmohammadi Khorrami, and M. Ghahraman Afshar, "Genetic algorithm based artificial neural network and partial least squares regression methods to predict of breakdown voltage for transformer oils samples in power industry using ATR-FTIR spectroscopy," *Spectrochimica Acta Part A: Molecular and Biomolecular Spectroscopy*, vol. 273, Article ID 120999, 2022.

[28] X. Zhang, L. Chen, Y. Sun, Y. Bai, B. Huang, and K. Chen, "Determination of zinc oxide content of mineral medicine calamine using near-infrared spectroscopy based on MIV and BP-ANN algorithm," *Spectrochimica Acta Part A: Molecular and Biomolecular Spectroscopy*, vol. 193, pp. 133–140, 2018.

[29] D. Pérez-Marín, A. Garrido-Varo, J. E. Guerrero, and J. C. Gutiérrez-Estrada, "Use of artificial neural networks in near-infrared reflectance spectroscopy calibrations for predicting the inclusion percentages of wheat and sunflower meal in compound feedingstuffs," *Applied Spectroscopy*, vol. 60, no. 9, pp. 1062–1069, 2006.

[30] Association of Official Analytical Chemists (Aoac), *Official Methods of Analysis*, Association of Official Analytical Chemists, Arlington, VA, USA, 20th edition, 2016.

[31] P. J. Van Soest, J. B. Robertson, and B. A. Lewis, "Methods for dietary fiber, neutral detergent fiber, and nonstarch polysaccharides in relation to animal nutrition," *Journal of Dairy Science*, vol. 74, no. 10, pp. 3583–3597, 1991.

[32] Association of Official Analytical Chemists (Aoac), *Official Methods of Analysis*, Association of Official Analytical Chemists, Arlington, VA, USA, 17th edition, 2000.

[33] A. Hristov, M. Harper, G. Roth et al., "Effects of ensiling time on corn silage neutral detergent fiber degradability and relationship between laboratory fiber analyses and in vivo digestibility," *Journal of Dairy Science*, vol. 103, no. 3, pp. 2333–2346, 2020.

[34] C. J. Richards, J. F. Pedersen, R. A. Britton, R. A. Stock, and C. R. Krehbiel, "In vitro starch disappearance procedure modifications," *Animal Feed Science and Technology*, vol. 55, no. 1-2, pp. 35–45, 1995.

[35] Y. L. Wang, W. K. Wang, Q. C. Wu et al., "In situ rumen degradation characteristics and bacterial colonization of corn silages differing in ferulic and p-coumaric acid contents," *Microorganisms*, vol. 10, no. 11, p. 2269, 2022.

[36] Y. Ma, M. Z. Khan, Y. Liu et al., "Analysis of nutrient composition, rumen degradation characteristics, and feeding value of Chinese rye grass, barley grass, and naked oat straw," *Animals*, vol. 11, no. 9, p. 2486, 2021.

[37] L. Qiu, M. Zhang, A. S. Mujumdar, and L. Chang, "Convenient use of near-infrared spectroscopy to indirectly predict the antioxidant activitiy of edible rose(Rose chinensis Jacq "Crimsin Glory" H.T.)petals during infrared drying," *Food Chemistry*, vol. 369, Article ID 130951, 2022.

[38] A. Chebil, B. H. Hurd, N. Mtimet, B. Dhehibi, and W. Bilel, "Economic Impact of Climate Change on Tunisian Agriculture: The Case of Wheat," *Vulnerability Of Agriculture, Water And Fisheries To Climate Change*, pp. 110–130, Springer, Berlin, Germany, 2014.

[39] A. Jonker and P. Yu, "The occurrence, biosynthesis, and molecular structure of proanthocyanidins and their effects on legume forage protein precipitation, digestion and absorption in the ruminant digestive tract," *International Journal of Molecular Sciences*, vol. 18, no. 5, p. 1105, 2017.

[40] A. Jonker and P. Yu, "The role of proanthocyanidins complex in structure and nutrition interaction in alfalfa forage," *International Journal of Molecular Sciences*, vol. 17, no. 5, p. 793, 2016.

[41] L. M. E. Mammi, G. Buonaiuto, F. Ghiaccio et al., "Combined inclusion of former foodstuff and distiller grains in dairy cows ration: effect on milk production, rumen environment, and fiber digestibility," *Animals*, vol. 12, p. 3519, 2022.

[42] G. Buonaiuto, A. Palmonari, F. Ghiaccio et al., "Effects of complete replacement of corn flour with sorghum flour in dairy cows fed Parmigiano Reggiano dry hay-based ration," *Italian Journal of Animal Science*, vol. 20, no. 1, pp. 826–833, 2021.

[43] D. Cavallini, A. Palmonari, L. Mammi, F. Ghiaccio, G. Canestrari, and A. Formigoni, "Evaluation of fecal sampling time points to estimate apparent nutrient digestibility in lactating Holstein dairy cows," *Frontiers in Veterinary Science*, vol. 9, Article ID 1065258, 2022.

[44] A. Palmonari, D. Cavallini, C. J. Sniffen et al., "In vitro evaluation of sugar digestibility in molasses," *Italian Journal of Animal Science*, vol. 20, no. 1, pp. 571–577, 2021.

[45] P. P. Subedi and K. B. Walsh, "Assessment of sugar and starch in intact banana and mango fruit by SWNIR spectroscopy," *Postharvest Biology and Technology*, vol. 62, no. 3, pp. 238–245, 2011.

[46] D. F. Tang, Z. G. Chen, F. Li et al., "Construction of a near-infrared prediction model for nutrient content in different parts (tissues) of corn silage," *Pratacultural Science*, vol. 38, no. 9, pp. 1753–1761, 2021.

[47] L. Xing, L. J. Chen, and L. J. Han, "Rapid analysis of layer manure using near-infrared reflectance spectroscopy," *Poultry Science*, vol. 87, no. 7, pp. 1281–1286, 2008.

[48] C. S. Wang, *Determination and Prediction of Metabolizable Energy Value and Amino Acids Availability of Different Source Corn and Soybean Meal in Laying Hens*, Sichuan Agricultural University, Yaan, China, 2014.

[49] P. J. Werbos, *Beyond Regression: New Tools for Prediction and Analysis in the Behavioural Sciences*, Harvard University, Boston, MA, USA, 1974.

[50] D. E. Rumelhart, G. E. Hinton, and R. J. Williams, "Learning representations by back-propagating errors," *Nature*, vol. 323, no. 6088, pp. 533–536, 1986.

[51] P. Williams, *Near-infrared Technology – Getting the Best Out of Light: A Short Course in the Practical Implementation of Near-Infrared Spectroscopy for the User*, Process Design Kit, Draper, UT, USA, 2nd edition, 2004.

[52] H. Yang, J. Jin, F. Hou, X. He, and Y. Hang, "An ANN-based method for predicting Zhundong and other Chinese coal slagging potential," *Fuel*, vol. 293, Article ID 120271, 2021.

[53] X. Niu, Z. Zhao, K. Jia, and X. Li, "A feasibility study on quantitative analysis of glucose and fructose in lotus root powder by FT-NIR spectroscopy and chemometrics," *Food Chemistry*, vol. 133, no. 2, pp. 592–597, 2012.